Published in final edited form as:
Science. 2011 April 8; 332(6026): 247–251. doi:10.1126/science.1201678.

AMP-Activated Protein Kinase Regulates Neuronal Polarization by Interfering with PI 3-Kinase Localization

Stephen Amato[1], **Xiuxin Liu**[2,*], **Bin Zheng**[3,4,*], **Lewis Cantley**[3,4], **Pasko Rakic**[2], and **Heng-Ye Man**[1,†]

[1]Department of Biology, Boston University, 5 Cummington Street, Boston, MA 02215, USA.

[2]Department of Neurobiology and Kavli Institute for Neuroscience, Yale University School of Medicine, New Haven, CT 06510, USA.

[3]Division of Signal Transduction, Beth Israel Deaconess Medical Center, Boston, MA 02115, USA.

[4]Department of Systems Biology, Harvard Medical School, Boston, MA 02115, USA.

Abstract

Axon-dendrite polarization is crucial for neural network wiring and information processing in the brain. Polarization begins with the transformation of a single neurite into an axon and its subsequent rapid extension, which requires coordination of cellular energy status to allow for transport of building materials to support axon growth. We found that activation of the energy-sensing adenosine 5′-monophosphate (AMP)–activated protein kinase (AMPK) pathway suppressed axon initiation and neuronal polarization. Phosphorylation of the kinesin light chain of the Kif5 motor protein by AMPK disrupted the association of the motor with phosphatidylinositol 3-kinase (PI3K), preventing PI3K targeting to the axonal tip and inhibiting polarization and axon growth.

Morphological polarization sets the foundation for synapse formation and efficient information transfer in the brain. Polarization is initiated by the selective rapid growth of a single neurite that will eventually differentiate into an axon, whereas the remaining sister neurites become dendrites. The scale of axon growth during neuronal polarization requires both a large energy supply to support increased protein and membrane synthesis and extremely active intracellular delivery (1). Cellular energy status could thus be a key factor in initiating axon outgrowth and polarity formation. In all cell types, including neurons, the adenosine 5′-monophosphate (AMP)–activated protein kinase (AMPK) signaling cascade measures bioenergy homeostasis, with its activity level inversely related to energy sufficiency (2), and is implicated in brain development (3).

To investigate the role of AMPK activity in neuronal polarization, we assessed the effect of the AMPK-specific agonists 5-amino 4-imidazolecarboxamide riboside (AICAR) or metformin in newly plated hippocampal neurons (4). AMPK activation, as indicated by

†To whom correspondence should be addressed. hman@bu.edu.
*These authors contributed equally to this work.

Supporting Online Material
www.sciencemag.org/cgi/content/full/science.1201678/DC1
Materials and Methods
Figs. S1 to S21
References and Notes

phosphorylation at Thr^{172}, occurred rapidly and was reversible after incubation with AICAR or metformin. AMPK signaling could be blocked by a selective antagonist, compound C (CC), and was accompanied by phosphorylation of a major AMPK target, acetyl–coenzyme A–carboxylase (ACC) (Fig. 1, A to C). To examine AMPK activity on polarization, we treated cultured hippocampal neurons during the transition from stage 2 to stage 3, a critical period in which rapid axonal growth and polarization occur (5) (Fig. 1D). In cultures incubated with AICAR or metformin, we observed a significant reduction in the number of neurons possessing a typical elongated axon (Fig. 1, E to J). In addition, a mild or transient AMPK activation inhibited polarization (figs. S1 and S2). AICAR-treated neurons displayed no significant change in both average length and rate of growth of nonaxonal minor neurites (Fig. 1H and fig. S3, A to D), whereas the growth of axon-like neurites and total neurite length was markedly reduced (Fig. 1, I and J). Neurons treated immediately after plating also showed no defect in minor neurite formation or growth (fig. S3, E to H). The specific suppression of axonal, but not minor neurites, together with the lack of propidium iodide labeling (fig. S4), indicates that the AICAR effect did not result from cell damage.

To confirm that the effect on polarity was directly mediated via AMPK, we transfected neurons with either wild-type (WT) or a kinase dead (KD) mutant AMPK (D157A, mutation of Asp^{157} to Ala) (Fig. 1, K and L). Overexpression of AMPK-WT alone caused a reduction in polarity that was further exaggerated by AICAR. In contrast, neurons expressing AMPK-KD established morphological polarity despite AICAR treatment, ruling out potential off-target effects of AICAR. Furthermore, expression of a constitutively active AMPK mutant (AMPK-CA) inhibited neuronal polarity and was not affected by AICAR(fig. S5). In line with the role of AMPK in axon initiation, progression into polarization stage 3 was accompanied by a drop in AMPK activity that remained stable throughout stage 3 (figs. S6 and S7). AICAR-induced AMPK phosphorylation was largely limited to the soma (fig. S8). Additionally, control cells displayed a mutually exclusive spatial distribution of MAP2 and Tau-1, markers for dendrite and axon, respectively, AICAR-treated neurons displayed amixed distribution pattern (fig. S9), indicating that AMPK activity altered both molecular and morphological polarity. Because AICAR-induced AMPK activation is reversible (Fig. 1A), we assessed whether the effect of AMPK on polarity was temporary. Neurons failed to establish polarity even 2 days after the removal of treatment (fig. S10), suggesting an irreversible effect. Furthermore, incubation of polarized stage 3 neurons with AICAR for 48 hours did not affect molecular polarity or axon length (fig. S11), excluding the possibility of a reversal in polarization.

The phosphatidylinositol 3-kinase (PI3K) signaling cascade is necessary for axonal neurite growth during polarization (6, 7). We wondered whether AMPK signaling might lead to an inhibition of the PI3K/Akt pathway. Instead, AICAR caused a substantial increase in total Akt phosphorylation (Fig. 2A and fig. S12), which was blocked by the PI3K inhibitor LY294002 (30 μM) (Fig. 2B). LY294002 showed no effect on AICAR-induced AMPK activation, indicating that PI3K functions downstream of AMPK to regulate Akt activity.

During neuronal polarization, PI3K and Akt activity becomes selectively enriched at the tip of a single nascent neurite, signaling the progression from nonpolarized stage 2 to polarizing stage 3 (7). We reasoned that AMPK signaling might disrupt the subcellular localization of PI3K. In early stage 3 neurons, AICAR treatment induced a marked increase in pAkt immunointensity within the soma (Fig. 2, D and H). However, unlike control cells that showed enhanced pAkt distribution at the tip of a single neurite, AICAR-treated neurons revealed no tip enrichment (Fig. 2, D to H, and fig. S13). Similarly, single-tip enrichment of the PI3K regulatory subunit p85 (fig. S14) and the PI3K-regulated polarity protein mPar3 (7, 8) (fig. S15) was also abolished by AICAR. In addition, we examined the localization of the Akt-derived pleckstrin homology (PH) domain fused to enhanced green fluorescent protein

(PH-EGFP) to indicate PI3K activity (9). Live imaging showed stable PH-EGFP localization at the tip of control axons, whereas 30-min AICAR treatment resulted in a retraction of PH-EGFP from the axon tip (Fig. 2J). Because PI3K acted downstream of AMPK (Fig. 2B), we attempted to rescue polarity by increasing PI3K activity. Most of the constitutively active PI3K (PI3K-CA) neurons polarized successfully despite enhanced AMPK activation (fig. S16), confirming the role of PI3K in AMPK-mediated polarity inhibition.

To explore whether AMPK activity alters motor-mediated tip transport of PI3K, we examined the involvement of kinesin I (Kif5), a plus end–directed molecular motor with an important role in axonal transport (10, 11) and cell polarity (12). Kif5 is also preferentially localized to the neurite tip of the future axon (13). Co-immunoprecipitation with stage 3 neuron lysates revealed an association of p85 with the cargo-binding kinesin light chain (KLC) (14–16), which was disrupted by AICAR (figs. S17A and S18). We identified two AMPK-dependent phosphorylation sites in KLC2, Ser^{539} and Ser^{575} (Fig. 3A and fig. S17, B and C). However, KLC2 double phosphorylation site mutation (KLC2-DM) failed to interact with p85 regardless of AMPK activation (Fig. 3B), perhaps due to tertiary-structure changes that interfered with p85 binding (17). Nevertheless, expression of KLC2-DM resulted in a loss of p85 at the tip independent of AMPK activation, consistent with the inability of KLC2-DM to interact with PI3K (Fig. 3, C to E). Thus, KLC2 acts as a kinesin motor adaptor for PI3K transport to the axon tip. Consequently, neurons expressing KLC2-DM failed to establish polarity regardless of AMPK activation state (Fig. 3, F and G). Moreover, coexpression of PI3K-CA with KLC-DM rescued neuronal polarization to control levels (fig. S19), confirming that the KLC-DM effect was indeed due to a reduced PI3K activity at the neurite tip.

To determine the effect of AMPK activation on polarity in a more physiological setting, we prepared organotypic brain slice cultures from embryonic day 14 (E14) mice and used retroviral infection to express EGFP in newly divided neurons (18) (Fig. 4A). In brain slices, AICAR incubation induced similar activation of AMPK and Akt pathways (fig. S20). In control slices, GFP-expressing neurons showed a typical basal axon and multiple apical dendrites derived from a single dendritic base (Fig. 4B). AICAR-treated neurons displayed no axon or possessed only a very short rudimentary neurite at the axonal pole and atypical dendrite patterning (Fig. 4, C to F). To further confirm the role of AMPK activity, we electroporated E15.5 mouse cortex in utero with Tα-1 Venus EGFP combined with AMPK-KD (Fig. 4, G to M). There was no discernable difference between neurons expressing EGFP alone and those coexpressing AMPK-KD. AICAR-treated neurons were characterized by several dendritic processes grown directly from the soma protruding in multiple directions and by irregular cell bodies, hallmarks of multipolar nonpolarized neurons in vivo (19–21). In contrast, a polarized morphology in AMPK-KD–expressing neurons was successfully established, with typical axon-dendrite bipolar neurites and a more elongated soma, despite AICAR treatment. Additionally, an ischemic challenge in cultured neurons induced an AMPK-dependent suppression of cell polarization (fig. S21, A to D), supporting an involvement of this energy-sensing pathway in patho-physiological conditions.

Here we have identified a crucial role of the bioenergy-sensing pathway in axon initiation, neuronal polarization, and differentiation into axons or dendrites. The AICAR effect on polarization was abolished by introduction of kinase-dead AMPK and mimicked by constitutively active AMPK, suggesting the requirement for AMPK activation. In native tissues and the brain, liver kinase B1 (LKB1) and calmodulin-dependent protein kinase kinase β (CaMKKβ) are major upstream activators of AMPK (22). LKB1 mediates axon initiation through SAD kinase activation (23, 24). However, LKB1 knockout had no effect on AMPK phosphorylation within the cortex (23). Furthermore, suppression of CaMKK activity inhibits neurite growth (25, 26). Thus, the upstream signaling molecules involved in

the observed AMPK effect remain unclear. Because AMPK activity is coupled to AMP/ATP ratio, regulation of AMPK by the upstream kinases should vary depending on energy status. In addition, given the large number of downstream targets, LKB1- or CaMKKβ-dependent cellular responses can be attained with substrates other than AMPK signaling. Indeed, transforming growth factor–β (TGF-β) signaling can lead to a similar phenotype in neuromorphogenesis (27), indicating the existence of multiple signaling pathways for neuronal polarization.

The AMPK effect on polarity was accompanied by a loss of axon-tip enrichment of several signaling components, including PI3K, p-Akt, and mPar3. In contrast to a reduced function at the neurite tip, PI3K and Akt activities at the total cellular level were greatly increased during AMPK activation. Under reduced-energy conditions that lead to AMPK activation, entry of glucose should be facilitated in order to increase ATP production (28). Perhaps the observed increase in PI3K/Akt activity during AICAR treatment facilitates increased glucose uptake (29). PI3K dislocation from the neurite tip may result from a failure in its motor-mediated delivery, due to AMPK-dependent phosphorylation on KLC. PI3K might be transported via direct P85-KLC interaction, similar to the delivery of collapsin response mediator protein–2 (CRMP-2) (15), or via indirect association through an intermediate molecule.

Supplementary Material

Refer to Web version on PubMed Central for supplementary material.

Acknowledgments

We thank H. R. Luo for providing EGFP-PH, K. Hasimoto-Torii for GFP virus, and J. Asara for assistance with mass spectrometry. This research was supported by MH07907 (H.-Y.M), GM56203 and GM41890 (L.C.C.), K99CA133245 (B.Z.), the Kavli Institute (P.R.), and a NAAR/Autism Speaks fellowship (X.L.).

References and Notes

1. Jareb M, Banker G. J. Neurosci. 1997; 17:8955. [PubMed: 9364043]
2. Hardie DG, Hawley SA, Scott JW. J. Physiol. 2006; 574:7. [PubMed: 16644800]
3. Dasgupta B, Milbrandt J. Dev. Cell. 2009; 16:256. [PubMed: 19217427]
4. Sabina RL, Patterson D, Holmes EW. J. Biol. Chem. 1985; 260:6107. [PubMed: 3997815]
5. Dotti CG, Sullivan CA, Banker GA. J. Neurosci. 1988; 8:1454. [PubMed: 3282038]
6. Ménager C, Arimura N, Fukata Y, Kaibuchi K. J. Neurochem. 2004; 89:109. [PubMed: 15030394]
7. Shi SH, Jan LY, Jan YN. Cell. 2003; 112:63. [PubMed: 12526794]
8. Kemphues K. Cell. 2000; 101:345. [PubMed: 10830161]
9. Jia Y, et al. Immunity. 2007; 27:453. [PubMed: 17825589]
10. Ferreira A, Niclas J, Vale RD, Banker G, Kosik KS. J. Cell Biol. 1992; 117:595. [PubMed: 1533397]
11. Nakata T, Hirokawa N. J. Cell Biol. 2003; 162:1045. [PubMed: 12975348]
12. Nakata T, Hirokawa N. Sci. STKE. 2007; 2007:pe6. [PubMed: 17284724]
13. Jacobson C, Schnapp B, Banker GA. Neuron. 2006; 49:797. [PubMed: 16543128]
14. Gindhart JG Jr. Desai CJ, Beushausen S, Zinn K, Goldstein LS. J. Cell Biol. 1998; 141:443. [PubMed: 9548722]
15. Kimura T, et al. J. Neurochem. 2005; 93:1371. [PubMed: 15935053]
16. Verhey KJ, et al. J. Cell Biol. 2001; 152:959. [PubMed: 11238452]
17. Seppälä S, Slusky JS, Lloris-Garcerá P, Rapp M, von Heijne G. Science. 2010; 328:1698. [PubMed: 20508091]
18. Tashiro A, Zhao C, Gage FH. Nat. Protoc. 2007; 1:3049. [PubMed: 17406567]

19. LoTurco JJ, Bai J. Trends Neurosci. 2006; 29:407. [PubMed: 16713637]
20. Rakic P, Stensas LJ, Sayre E, Sidman RL. Nature. 1974; 250:31. [PubMed: 4210169]
21. Tabata H, Nakajima K. J. Neurosci. 2003; 23:9996. [PubMed: 14602813]
22. Hardie DG. Nat. Rev. Mol. Cell Biol. 2007; 8:774. [PubMed: 17712357]
23. Barnes AP, et al. Cell. 2007; 129:549. [PubMed: 17482548]
24. Shelly M, Cancedda L, Heilshorn S, Sumbre G, Poo MM. Cell. 2007; 129:565. [PubMed: 17482549]
25. Ageta-Ishihara N, et al. J. Neurosci. 2009; 29:13720. [PubMed: 19864584]
26. Wayman GA, et al. J. Neurosci. 2004; 24:3786. [PubMed: 15084659]
27. Yi JJ, Barnes AP, Hand R, Polleux F, Ehlers MD. Cell. 2010; 142:144. [PubMed: 20603020]
28. Russell RR 3rd. J. Clin. Invest. 2004; 114:495. [PubMed: 15314686]
29. Katagiri H, et al. J. Biol. Chem. 1996; 271:16987. [PubMed: 8663584]

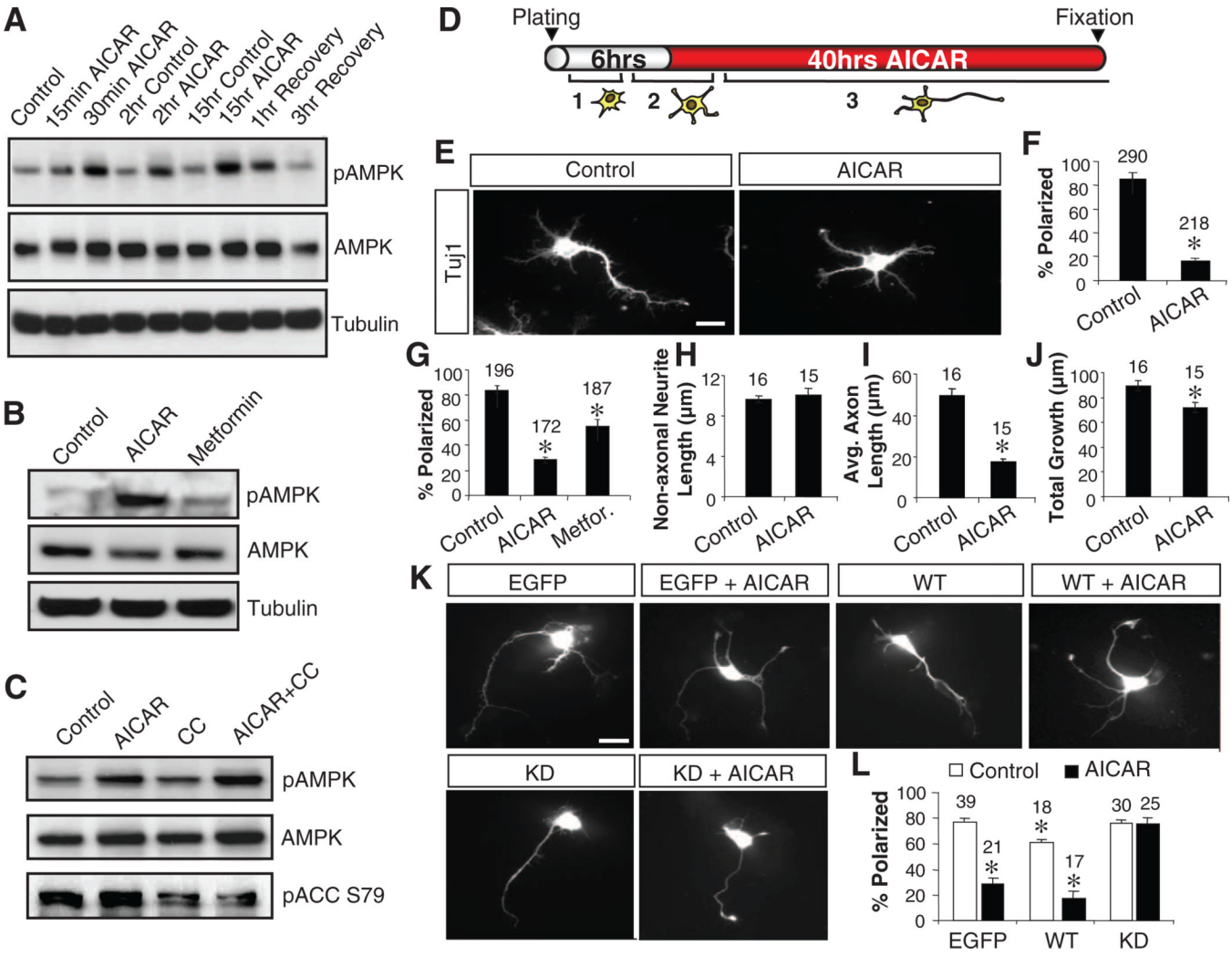

Fig. 1.

AMPK activation suppresses neuronal polarization in cultured hippocampal neurons. (**A**) Time course for AMPK activation (pAMPK) by AICAR (2 mM) in day 1 in vitro (DIV1) hippocampal neurons. (**B**) Incubation of DIV1 neurons with AICAR and metformin (200 µM) on AMPK activation. (**C**) Neurons were pretreated with compound C (CC) (20 µM) for 1 hour followed by 30-min incubation with AICAR. (**D**) Illustration of AICAR treatment paradigm with corresponding polarization stages. (**E** to **G**) Effect of AMPK activation by AICAR and metformin on neuronal polarization. (**H** to **J**) Measurement of nonaxonal neurite length, axon length, and the total growth. (**K** and **L**) Expression of wild-type (WT) or kinase-dead (KD) AMPK on neuronal polarity. Cell numbers of statistical analysis are indicated at the top of bar graphs. *$P < 0.05$, two-population Student's t test [(F) and (H) to (J)], or analysis of variance (ANOVA) with Tukey post-test [(G) and (L)]. Scale bar, 20 µm.

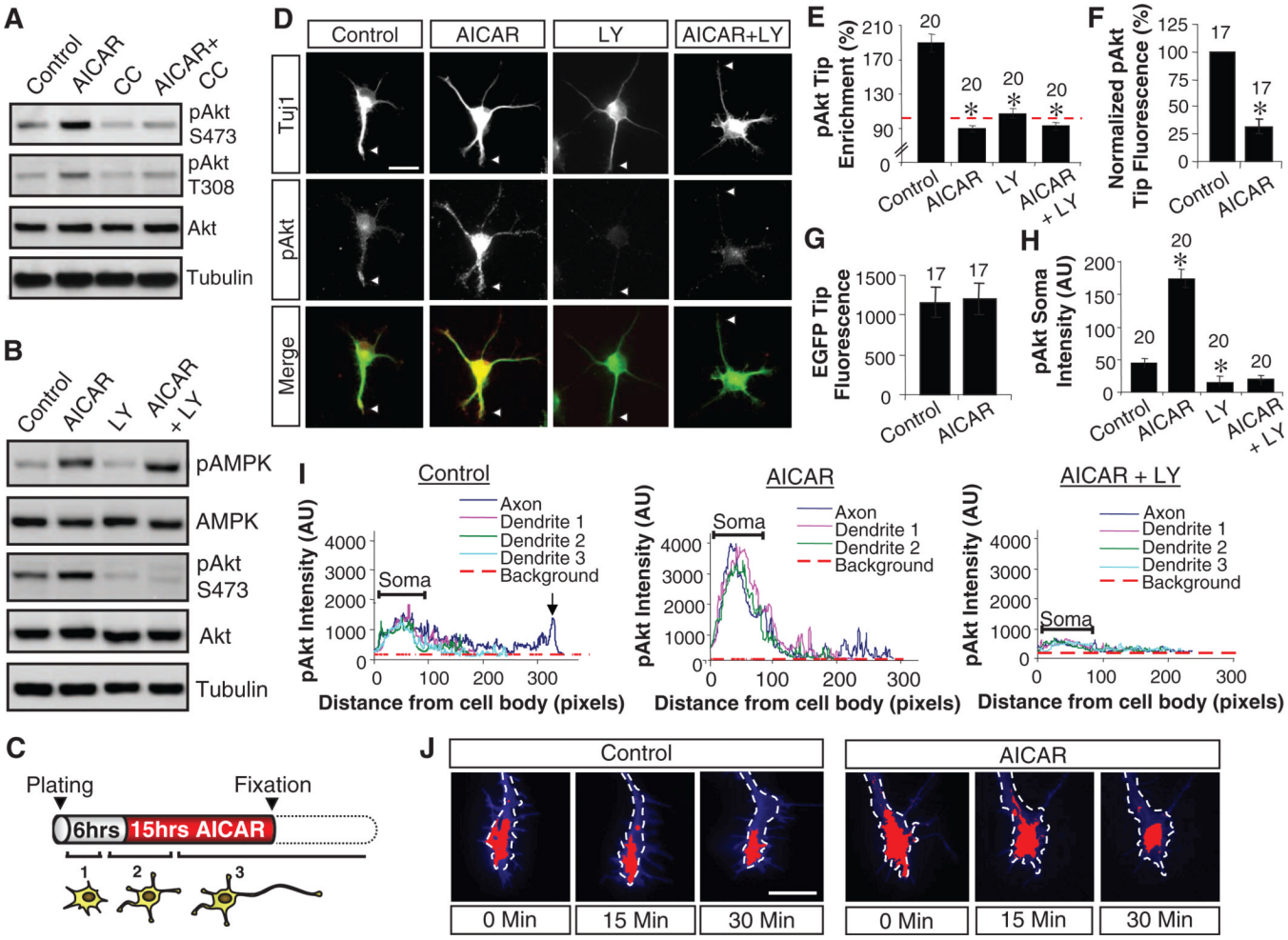

Fig. 2.

AMPK activation disrupts tip localization of active Akt. (**A** and **B**) AICAR treatment on PI3K-mediated Akt phosphorylation in DIV1 neurons. (**C**) Illustration of AICAR treatment paradigm. (**D**)Hippocampal neurons treated with AICAR and LY294002 (LY), respectively, or together for 15 hours, immunostained for phospho-Akt (Ser^{473}) and neuronal marker Tuj1. Scale bar, 20 μm. (**E**) Quantification of tip fluorescence intensity normalized to shaft intensity. (**F**) Normalization of tip pAkt intensity to tip area indicated by EGFP. (**G**) EGFP intensity at axonal tip. (**H**) Quantification of pAkt soma intensity. (**I**) Plot profile of p-Akt signals from the soma to neurite tips. Dashed line indicates background intensity. (**J**) Live imaging of PH-EGFP in stage 3 neurons. *$P < 0.05$, ANOVA with Tukey post-test [(E) and (H)], or two-population Student's *t* test [(F) and (G)]. Scale bar, 10 μm.

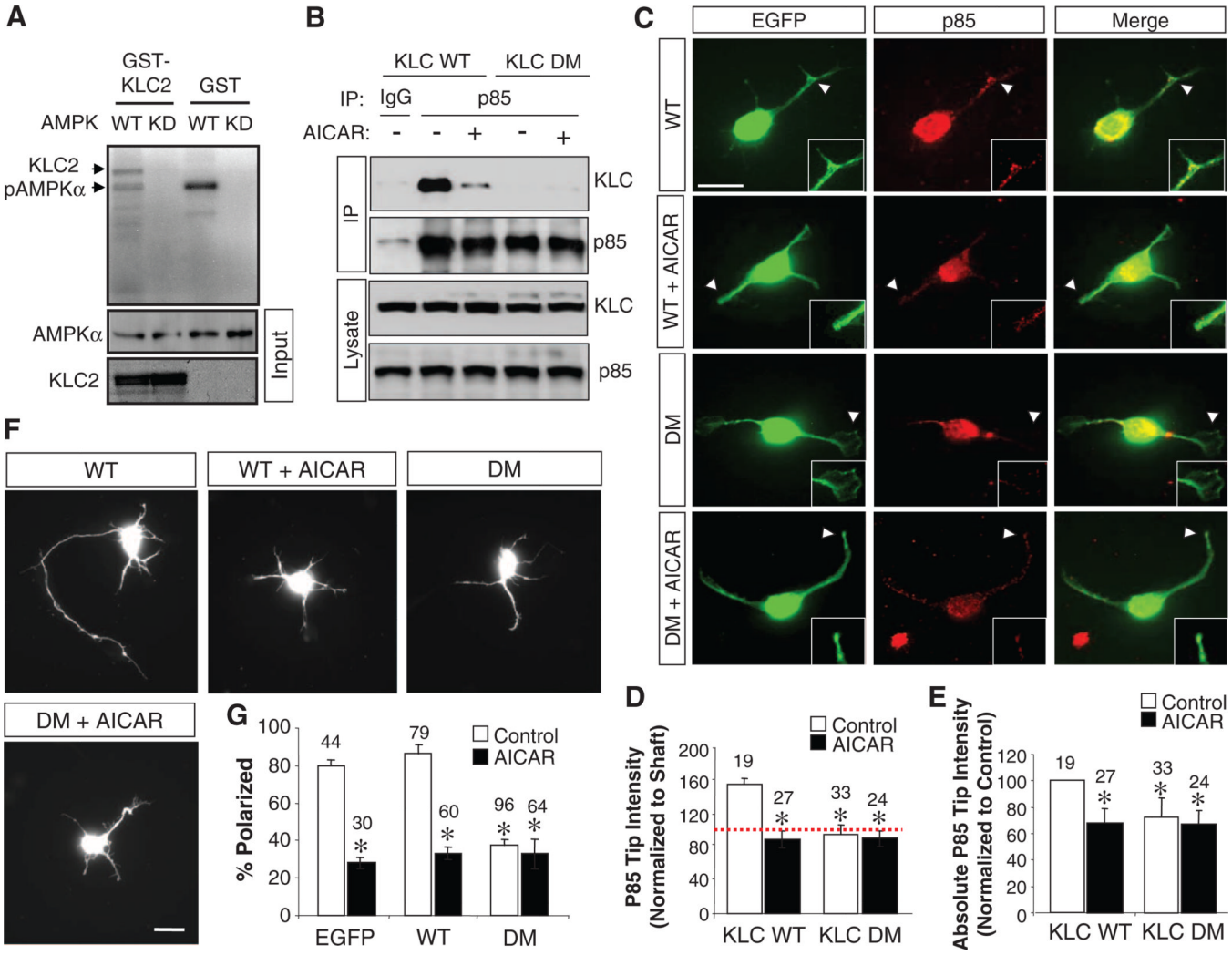

Fig. 3.

Association of KLC2 and p85 is required for PI3K tip enrichment and neuronal polarity. (**A**) In vitro phosphorylation of KLC2 by AMPK. Purified GST-KLC2 was incubated with wild-type (WT) or kinase dead (KD) AMPK catalytic α1 subunit in the presence of P^{32}-labeled ATP. Positive radioactivity was observed in KLC2 and AMPK α1 subunit, indicating phosphorylation of KLC2 and autophosphorylation of AMPK. GST (glutathione *S*-transferase) was used as a control. (**B**) Immunoprecipitation of GFP-p85 in human embryonic kidney cells expressing GFP-p85 together with wild-type or mutant Myc-KLC2 (DM). (**C** to **E**) Immunostaining of p85 in stage 3 hippocampal neurons transfected with EGFP alone or together with either the WT or DM KLC2. (**F** and **G**) AICAR treatment on neurons expressing EGFP together with WT or DM KLC2. **P* < 0.05, ANOVA with Tukey post-test. Scale bar, 20 μm.

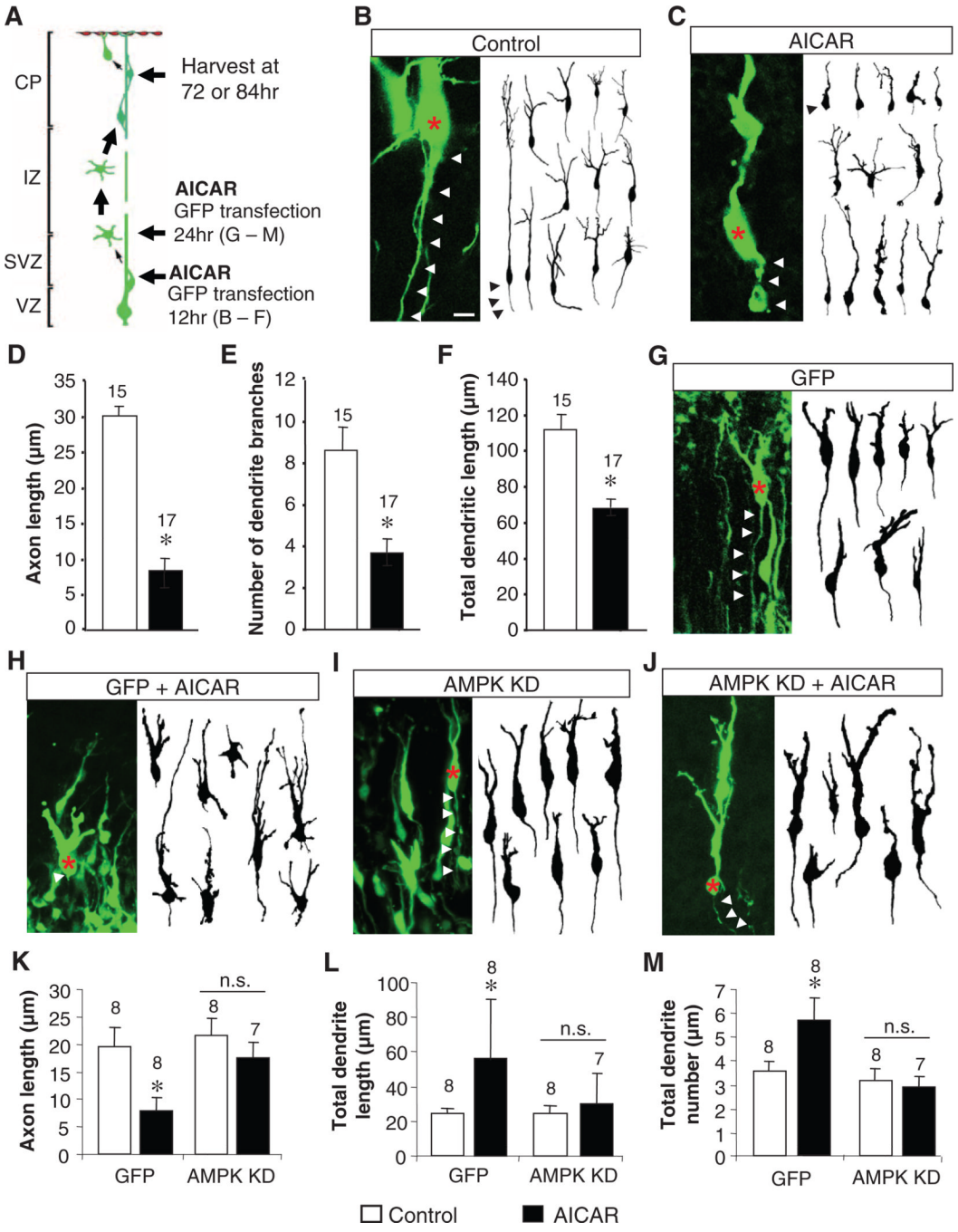

Fig. 4.

AMPK activation disrupts neuronal polarization in organotypic slice culture. (**A**) Illustration of experimental design and stages of neuronal polarization. (**B** to **F**) Cortical brain slices prepared from E14 mice were infected with CAG-GFP retrovirus to indicate newborn neurons and treated with AICAR (2 mM, 72 hours). (**G** to **M**) The embryonic brain (E15.5) was in utero–electroporated with EGFP with or without AMPK-KD, and brain slices were prepared for AICAR incubation (48 hours). Arrowheads and stars indicate axonal segment and the soma, respectively. *$P < 0.05$, two-population Student's *t* test [(D) to (F)], or ANOVA with Tukey post-test [(K) to (M)]. Scale bar, 10 µm.